Quantum Vacuum Energy in Graphs and Billiards

L. Kaplan

Department of Physics, Tulane University, New Orleans, Louisiana 70118, USA

Abstract. The vacuum (Casimir) energy in quantum field theory is a problem relevant both to new nanotechnology devices and to dark energy in cosmology. The crucial question is the dependence of the energy on the system geometry under study. Despite much progress since the first prediction of the Casimir effect in 1948 and its subsequent experimental verification in simple geometries, even the sign of the force in nontrivial situations is still a matter of controversy. Mathematically, vacuum energy fits squarely into the spectral theory of second-order self-adjoint elliptic linear differential operators. Specifically, one promising approach is based on the small-t asymptotics of the cylinder kernel $e^{-t\sqrt{H}}$, where H is the self-adjoint operator under study. In contrast with the well-studied heat kernel e^{-tH}, the cylinder kernel depends in a non-local way on the geometry of the problem. We discuss some results by the Louisiana-Oklahoma-Texas collaboration on vacuum energy in model systems, including quantum graphs and two-dimensional cavities. The results may shed light on general questions, including the relationship between vacuum energy and periodic or closed classical orbits, and the contribution to vacuum energy of boundaries, edges, and corners.

Keywords: Casimir force, vacuum energy, quantum graphs, quantum billiards
PACS: 03.70.+k, 11.10.Gh, 11.80.La, 03.65.Sq

1. INTRODUCTION

Since Casimir's famous calculation in 1948 showing an attractive force between parallel conducting plates due to vacuum fluctuations of the electromagnetic field [1], forces associated with vacuum energy in quantum field theory have been studied in a wide variety of contexts [2]. These range from the bag model of the nucleon [3], to cosmology [4], to stabilization of brane world models [5], and to practical applications in micro- and nano-electromechanical systems [6].

Of course, the calculational details in specific applications will depend on the system dimension, the nature of the relevant quantum fluctuating field (e.g., a vector electromagnetic field), and the detailed boundary conditions (e.g., ones that properly take into account the finite plasma frequency in the electromagnetic case). In the examples considered here, we bypass these application-specific details and instead consider a toy model of a scalar field, usually with Dirichlet or Neumann boundary conditions. As we will see, these simple examples will help to elucidate important general questions concerning Casimir forces that are independent of the specific context. These questions relate to proper regularization and renormalization of the formally infinite vacuum energy, the relation of Casimir forces to periodic and closed classical paths, and the role of boundaries, edges, and corners.

Formally, the vacuum energy of a scalar field is given by $\frac{\hbar}{2}\sum_n \omega_n$, where ω_n are

the eigenfrequencies, given by solutions of $-\nabla^2\varphi_n = \frac{\omega_n^2}{c^2}\varphi_n$ with the relevant boundary conditions. In the following, we work in units where $\hbar = c = 1$. Of multiple methods of regularizing the infinite vacuum energy (including e.g., dimensional regularization), we focus here on the time-splitting regulator, associated with the cylinder kernel $T_t(x,y) = \langle x|e^{-\sqrt{-\nabla^2}t}|y\rangle$. Defining

$$E_t = -\frac{1}{2}\frac{\partial}{\partial t}\mathrm{Tr}\,T_t = \frac{1}{2}\sum_n \omega_n e^{-\omega_n t}\,, \tag{1}$$

the physical vacuum energy is given by taking the limit of E_t as $t \to 0$ if this limit exists (i.e. if the divergent terms can be shown to cancel).

2. VACUUM ENERGY IN QUANTUM GRAPHS

We begin by applying the above approach to quantum graphs, a class of one-dimensional models that have been widely used as approximations for the free-electron theory of conjugated molecules in chemistry, for quantum wire circuits in nanotechnology, and for photonic crystals in optics. More generally, quantum graphs provide a useful testing ground for investigating general questions about quantum chaos, scattering, and spectral theory. A good discussion may be found in a recent survey by Kuchment [7].

Mathematically, a quantum graph consists of one-dimensional bonds meeting at vertices, with the scalar field satisfying $-\nabla^2\varphi_n = \frac{\omega_n^2}{c^2}\varphi_n$ on each bond and prescribed boundary conditions at each vertex. For detailed presentations of the mathematical model, see Refs. [8, 9]. Vacuum energy in quantum graphs has been studied recently by Berkolaiko, Harrison, and Wilson [10]; here we show some results obtained by Fulling, Kaplan, and Wilson [11].

2.1. Pistons in One Dimension

The left panel of Figure 1 shows a simple line graph consisting of three bonds and four vertices. The two middle vertices are to be thought of as movable pistons, i.e. their position may change keeping the total length $L_1 + a + L_2$ fixed. The objective is to calculate the vacuum energy as a function of these positions, and thus to obtain a Casimir force acting on the pistons [12]. Focusing first on the bond of length a separating the pistons, we note that the eigenfrequencies are $\omega_n = n\pi/a$, where $n = 1, 2, \cdots$ for Dirichlet boundary conditions at the pistons. We then have

$$\begin{aligned} \mathrm{Tr}\,T_t &= \sum_{n=1}^{\infty} e^{-\pi n t/a} \\ &= \frac{e^{-\pi t/a}}{1 - e^{-\pi t/a}} \\ &= \frac{a}{\pi t} - \frac{1}{2} + \frac{\pi t}{12a} + O(t^2)\,, \end{aligned} \tag{2}$$

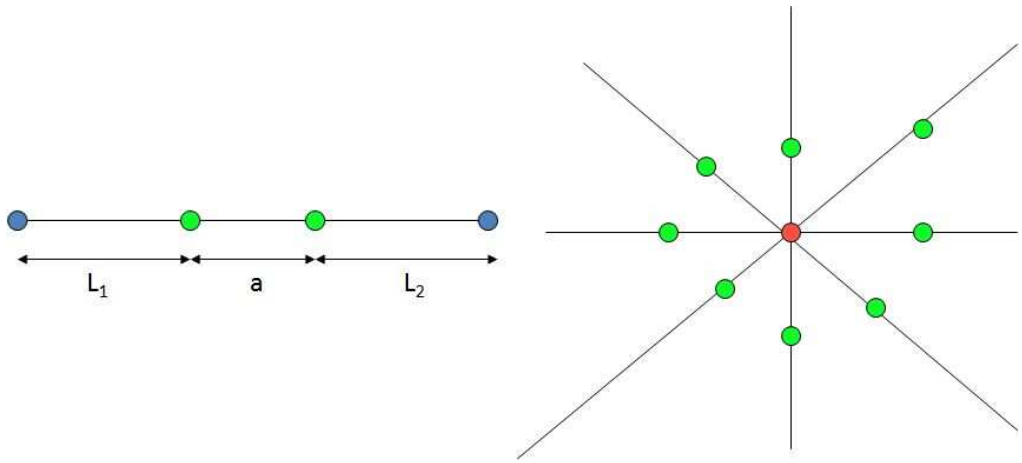

FIGURE 1. (Left) A line graph consisting of three bonds and four vertices. The two middle vertices are movable pistons. (Right) A star graph with $B = 8$ pistons.

and the regularized vacuum energy is

$$E_t = \frac{a}{2\pi t^2} - \frac{\pi}{24a} + O(t)\,. \tag{3}$$

Adding the vacuum energy from the other two segments, we find

$$E_t = \frac{L_1 + a + L_2}{2\pi t^2} - \frac{\pi}{24a} - \frac{\pi}{24L_1} - \frac{\pi}{24L_1} + O(t)\,. \tag{4}$$

Thus the divergent term corresponds to a geometry-independent constant energy density, and is unobservable since it will not contribute to a force on the piston. After safely discarding this constant energy shift, we may let $t \to 0$ and $L_{1,2} \to \infty$ and obtain the well-known finite, attractive force

$$F_{DD} \equiv -\frac{\partial E}{\partial a} = -\frac{\pi}{24a^2}\,. \tag{5}$$

The same result is obtained if Neumann boundary conditions obtain at each vertex ($\omega_n = n\pi/a$ with $n = 0, 1, 2, \cdots$). However, if one piston is Dirichlet and the other Neumann, the analogous calculation yields a repulsive force

$$F_{DN} = +\frac{\pi}{48a^2}\,. \tag{6}$$

Though simple, the calculations yield little or no insight as to why the force may be attractive in some situations and repulsive in others. To obtain such insight, we turn to an alternative perspective. We first note that

$$\mathrm{Tr}\, T_t = \int dx\, T_t(x,x)\,. \tag{7}$$

Now the free cylinder kernel in one dimension is

$$T_t^0(x,y) = \frac{t}{\pi}\frac{1}{(x-y)^2+t^2}\,. \tag{8}$$

Then $T_t(x,x)$ in a problem with boundaries is obtainable by the method of images as a sum over periodic and closed orbits:

$$T_t(x,x) = \mathrm{Re}\sum_p \frac{t}{\pi}\frac{A_p}{L_p^2+t^2} + \text{closed orbits}\,, \tag{9}$$

where p labels periodic orbits passing through x, L_p is the orbit length, and A_p is the product of scattering factors at vertices (e.g., -1 at a Dirichlet vertex and $+1$ at a Neumann vertex.) The expression arising from closed orbits (i.e. orbits starting and ending at x but with opposite momenta) is similar, and is omitted here because after integration over x, closed orbits in graphs may be shown to give zero contribution to the total energy. This is not the case in two- or three-dimensional billiards, as discussed in Section 3.

In our case, all periodic orbits in the region between the pistons are repetitions of the primitive periodic orbit of length $2a$. Separating out the zero-length orbit ($r = 0$) and taking the trace, we find

$$\mathrm{Tr}\, T_t = \int dx\, T_t(x,x) = \frac{t}{\pi}\frac{a}{t^2} + \mathrm{Re}\sum_{r=1}^{\infty}\frac{t}{\pi}\frac{4aA^r}{(2ra)^2+t^2}\,, \tag{10}$$

where r labels the repetition number and A is the product of scattering factors for the primitive two-bounce orbit.

The asymptotic $t \to 0$ behavior may now be analyzed term by term. We immediately see that all orbits of nonzero length make contributions $\sim t$ to the cylinder kernel, and thus finite $t-$independent contributions to the energy. The $t \to 0$ divergence is seen to be associated exclusively with the zero-length periodic orbits, which exist at every point x and yield the divergent but constant and geometry-independent energy density.

The periodic orbit sum converges. Differentiating $\mathrm{Tr}\, T_t$ with respect to t to obtain the vacuum energy and then with respect to a to obtain the force on a piston, we have

$$F = -\frac{1}{4\pi a^2}\sum_{r=1}^{\infty}\frac{A^r}{r^2}\,. \tag{11}$$

We note that $A = +1$ if the pistons are both Neumann or both Dirichlet, and $A = -1$ for mixed boundary conditions. Eq. (11) thus reproduces the results of Eqs. (5) and (6); moreover we see that the sign of the force arises from reflection phases, and is already correctly obtained if we consider only the phase associated with the shortest periodic orbit ($r = 1$).

2.2. Pistons in General Star Graphs

We turn our attention to star graphs, an example of which is pictured in the right panel of Fig. 1. A total of B line segments of large length L meet at the central vertex, where

the wave function satisfies Kirchhoff boundary conditions: (i) continuity $\varphi_j(0) = \varphi_k(0)$ for all $j,k = 1\cdots B$ and (ii) current conservation $\sum_{j=1}^{B} \varphi_j'(0) = 0$, where $\varphi_j'(0)$ is the outward derivative along bond j. Along each segment j, a piston is located at distance a_j from the central vertex, and the boundary condition imposed by the piston may be Dirichlet (reflection with phase -1), Neumann (reflection with phase $+1$), or reflection with an arbitrary phase $e^{i\theta_j}$ (to break time reversal symmetry). We will be interested in computing the dependence of the energy on the piston positions, i.e. in the Casimir force on the pistons.

We focus initially on the "interior" of our system, i.e. on the graph consisting of B bonds of length $a_1\cdots a_B$, and excluding the space beyond the pistons. For $B > 2$ and generic a_j, no analytic expression exists for the spectrum or for the vacuum energy, and a numerical approach must be employed. For a general quantum graph, the eigenfrequencies are given by solutions of a characteristic equation $\det h(\omega) = 0$ [8]; in the case of a star graph with irrationally related bond lengths a_j the relevant equation becomes

$$\sum_{j=1}^{B} \tan(\omega a_j + \theta_j) = 0\,, \tag{12}$$

where $\theta_j = 0$ or π for a Neumann or Dirichlet piston on bond j, respectively [11]. If we numerically obtain in this way all eigenfrequencies ω_n up to a cutoff $\omega_{\max}$, we may write

$$E_t^{\text{num}} = \frac{1}{2} \sum_{\omega_n < \omega_{\max}} \omega_n e^{-\omega_n t} = E_t + O(e^{-\omega_{\max} t})\,. \tag{13}$$

Since the error associated with omitting eigenfrequencies $\omega_n > \omega_{\max}$ is $O(e^{-\omega_{\max} t})$, we must consider $\omega_{\max} t \gg 1$.

Now we turn to the "outside," i.e. the segments $a_j \le x_j \le L$ located beyond the pistons. From Section 2.1 we know that the outside energy consists of finite terms that decay as $1/L$ and may therefore be neglected for large L, plus a divergent $1/t^2$ term associated with a geometry-independent constant energy density. The divergent terms, as before, will combine with the divergent part of the interior vacuum energy to yield a constant energy shift $BL/2\pi t^2$ proportional to the total length BL and independent of the piston positions. To obtain the physical forces on the pistons for large L we thus need only to subtract from the interior energy the divergence proportional to the total interior length $\sum_j a_j$. The physically observable energy is then given by

$$E_t^{\text{finite}} = E_t^{\text{num}} - E_t^{\text{Weyl}}\,, \tag{14}$$

where the divergence coming from integrating the Weyl density in one dimension $\rho(\omega) = \sum_j a_j/\pi$ between 0 and $\omega_{\max}$ is

$$E_t^{\text{Weyl}} = \left(\sum_{j=1}^{B} a_j\right) \cdot \frac{[1 - (\omega_{\max} t + 1)e^{-\omega_{\max} t}]}{2\pi t^2}\,. \tag{15}$$

Expressing the finite part of E_t as a power series,

$$E_t^{\text{finite}} = E_0 + \alpha_1 t + \alpha_2 t^2 + \cdots \tag{16}$$

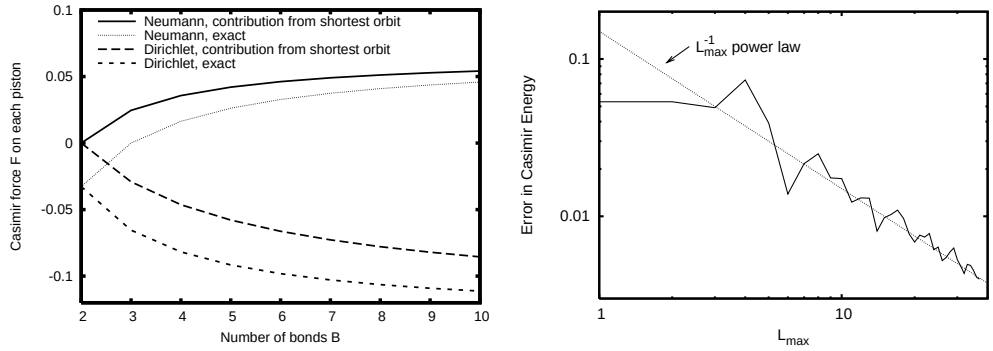

FIGURE 2. (Left) The force on a piston in a star graph with B bonds of length 1 and either Neumann or Dirichlet boundary conditions at each piston is computed using only repetitions of the shortest periodic orbit and compared with the exact answer. Positive values indicate repulsive forces. (Right) The difference between the exact Casimir energy E_0 and a periodic orbit sum including all orbits up to length $L_{\max}$ is shown for a star graph with four bonds of length 1.1, 1.6176, 1.2985, and 1.1159, and a Neumann piston at the end of each bond [11].

and numerically evaluating E_t^{finite} for several values of the cutoff t with $\omega_{\max}^{-1} \ll t \ll \min(a_j)$, we easily obtain the vacuum energy E_0 for any given star graph to any desired order of accuracy.

To attain a more physical understanding, we wish to compare the numerical results with periodic orbit sums. For example, taking all pistons to have Neumann boundary conditions and summing only over repetitions of the shortest periodic orbits (i.e., over orbits bouncing back and forth in a single bond), we obtain

$$E_N^{\text{shortest}} = \frac{\pi}{48}\left(1 - \frac{24\ln 2}{\pi^2 B} + \cdots\right)\sum_{j=1}^{B}\frac{1}{a_j}, \tag{17}$$

which for large B compares well to the analytic result $\frac{\pi}{48}\left(1-\frac{3}{B}\right)\frac{B}{a}$ for B *equal-length* bonds. Similar results are obtained in the Dirichlet case. As illustrated in the left panel of Figure 2, both repulsive behavior in the Neumann case and the attractive behavior in the Dirichlet case are well explained by considering only the shortest periodic orbit. For a better quantitative approximation we may add contributions from orbits of longer length. Figure 2 (right panel) shows the convergence to the numerically exact Caimir energy E_0 for a typical star graph with Neumann pistols. Here the error scales as $L_{\max}^{-1}$, where $L_{\max}$ is the length of the longest orbit included. For mixed Dirichlet or Neummann boundaries, or for arbitrary phases at the pistons, the convergence is shown to be $L_{\max}^{-3/2}$ [11].

3. VACUUM ENERGY IN RECTANGLES, PISTONS, AND PISTOLS

We now extend the approach of Section 2 to two-dimensional billiards (the extension to the three-dimensional case and the electromagnetic field is also straightforward [13].) An important motivation for this work [14] is to investigate the physical reality of the

outward force on the walls of a square or cubic box, as obtained by Lukozs using naive renormalization (i.e., by simply discarding infinite terms) and ignoring the outside of the box [15].

We begin with a rectangle of sides a and b. As for a line segment (Section 2.1), we can use the method of images to evaluate Tr T_t, and thus the regularized vacuum energy E_t. Each term in the image sum may be associated with a classical path leading from x to x in the rectangular, and these terms may be classified by the number of bounces the path makes off the vertical and horizontal walls. Periodic paths make an even number of bounces $2j$ off the vertical sides and an even number of bounces off the horizontal sides. The resulting contribution to the vacuum energy is

$$\begin{aligned} E_{t,\text{Periodic}} &= \frac{ab}{2\pi t^3} - \frac{ab}{2\pi}\sum_{k=1}^{\infty}(-1)^{\eta_{0k}}\frac{(2kb)^2-2t^2}{[t^2+(2kb)^2]^{5/2}} - \frac{ab}{2\pi}\sum_{j=1}^{\infty}(-1)^{\eta_{j0}}\frac{(2ja)^2-2t^2}{[t^2+(2ja)^2]^{5/2}} \\ &\quad -\frac{ab}{\pi}\sum_{j=1}^{\infty}\sum_{k=1}^{\infty}(-1)^{\eta_{jk}}\frac{(2ja)^2+(2kb)^2-2t^2}{[t^2+(2ja)^2+(2kb)^2]^{5/2}}\,, \end{aligned} \tag{18}$$

where η_{jk} is the number of Dirichlet bounces for a given orbit, and we have separated out the purely vertical and purely horizontal periodic orbits ($j=0$ and $k=0$, respectively), as well as the zero-length orbit $j=k=0$. As in the one-dimensional case, the zero-length orbit contributes a divergent but constant and geometry-independent energy density, i.e., a divergence proportional to the total area ab. Assuming all Neumann or all Dirichlet sides, so that all $\eta_{jk}=0$, we have

$$E_{t,\text{Periodic}} = \frac{ab}{2\pi t^3} - \frac{\zeta(3)}{16\pi}\left(\frac{a}{b^2}+\frac{b}{a^2}\right) - \frac{ab}{8\pi}\sum_{j=1}^{\infty}\sum_{k=1}^{\infty}\left(a^2j^2+b^2k^2\right)^{-3/2} + O(t^2)\,. \tag{19}$$

In contrast with the one-dimensional case, here the non-periodic closed orbits (ones that make an odd number of bounces off the horizontal sides, or an odd number of bounces off the vertical sides, or both), make a nonzero contribution to the total energy, including a divergent contribution proportional to the system perimeter. Combining periodic and non-periodic terms we obtain

$$\begin{aligned} E_t &= \frac{\text{Area}}{2\pi t^3} \mp \frac{\text{Perimeter}}{8\pi t^2} - \frac{\zeta(3)}{16\pi}\left(\frac{a}{b^2}+\frac{b}{a^2}\right) \\ &\quad - \frac{ab}{8\pi}\sum_{j,k=1}^{\infty}\left(a^2j^2+b^2k^2\right)^{-3/2} \pm \frac{\pi}{48}\left(\frac{1}{a}+\frac{1}{b}\right) + O(t^2)\,, \end{aligned} \tag{20}$$

where $\mp$ refers to Neumann or Dirichlet boundaries, respectively. Naively discarding the divergent terms and differentiating with respect to a we find an attractive force for $a \ll b$ (as expected in the limit of two infinite parallel plates), but a repulsive force for the square $a=b$.

The above analysis has two (related) problems: discarding divergent terms and ignoring the outside of the box. Both may be cured by considering a piston configuration [12], as discussed in Section 2 and illustrated in Figure 3 (Left). Adding contributions from

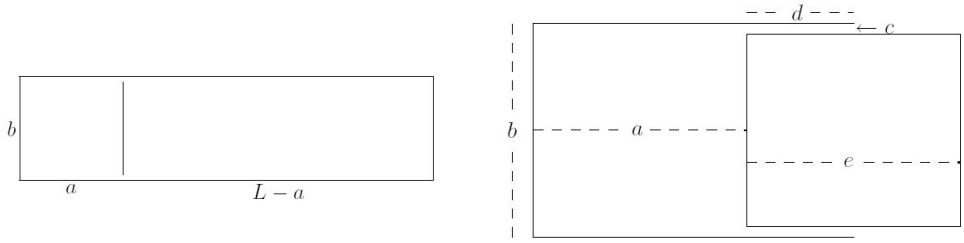

FIGURE 3. (Left) A piston in a rectangular box. (Right) A pistol configuration, consisting of a "barrel" and a "bullet."

the $a \times b$ rectangle and the $(L-a) \times b$ rectangle, we see that the divergent terms combine to yield contributions proportional to the total system area, and total boundary length, and thus independent of the position of the piston. Other than these divergent terms, the only contribution from the $(L-a) \times b$ rectangle that survives the $L \to \infty$ limit is $\frac{\zeta(3)}{16\pi}\left(\frac{L-a}{b^2}\right)$; combining this term with the finite part of Eq. (20) and differentiating with respect to a we obtain a finite Casimir force,

$$F_{\text{piston}} = \frac{\pi}{b^2} \sum_{j,k=1}^{\infty} k^2 K_1'\left(2\pi jk \frac{a}{b}\right) . \tag{21}$$

This force is always attractive (decaying exponentially for $a \gg b$ and reducing to the parallel plate limit for $a \ll b$).

Finally, to approach the original motivating situation of a box with a loose lid [15] and to address the question of what happens when the external shaft is not present, we consider the "pistol" configuration illustrated in the Right panel of Figure 3. Here all system dimensions other than possibly the gap c are assumed to be large compared to the ultraviolet cutoff t. We then use scaled variables $c = rt$, $a = st$, $b = ut$, $d = (\ell - s)t$, where $s, u, \ell \gg 1$, and for all Dirichlet boundaries obtain

$$\begin{aligned} E_{\text{pistol}} \;=\; & \frac{us}{\pi t} \sum_{k=1}^{\infty} \frac{1-2k^2u^2}{(1+4k^2u^2)^{5/2}} + \frac{us}{\pi t} \sum_{j=1}^{\infty} \frac{1-2j^2s^2}{(1+4j^2s^2)^{5/2}} \\ & + \frac{2us}{\pi t} \sum_{j=1}^{\infty} \sum_{k=1}^{\infty} \frac{1-2j^2s^2-2k^2u^2}{(1+4j^2s^2+4k^2u^2)^{5/2}} \\ & + \frac{s}{2\pi t} \sum_{j=1}^{\infty} \frac{-1+4j^2s^2}{(1+4j^2s^2)^2} + \frac{2r(\ell-s)}{\pi t} \sum_{k=1}^{\infty} \frac{1-2k^2r^2}{(1+4k^2r^2)^{5/2}} \end{aligned} \tag{22}$$

In the case of a narrow chamber, $a \ll b^{1/3}c^{2/3}$, we recover an attracive force $\sim 1/a^2$, as required in the parallel plate limit. In the opposite case of a long chamber, $a \gg b^{1/3}c^{2/3}$, we find that the gaps of width c dominate and we obtain an a-independent force that is attractive for $c > \alpha t$ and repulsive for $x < \alpha t$, where $\alpha \approx 0.5888$. This last situation, however, is least convincing physically, as we need to be in a regime where the gap dimension is smaller than the cutoff. See Ref. [14] for a detailed discussion.

4. GENERAL BILLIARDS

We note that the numerical approach to calculating the vacuum self-energy, applied to general quantum star graphs in Section 2.2, may be equally well applied to two- or three-dimensional systems, provided the spectrum may accurately be computed numerically up to some maximum frequency $\omega_{\max}$. Of course the appropriate Weyl term containing all $t \to 0$ divergences must be subtracted from the numerical sum (13) before the numerical limit $t \ll 1$ may be considered. For example in the case of the interior of a three-dimensional cylinder with polygonal cross sections and Dirichlet boundary conditions [16], Eq. (15) becomes

$$E_t^{\text{Weyl}}(t) = \frac{1}{2}\int_{-\infty}^{\infty}\frac{dk}{2\pi}\int_0^{\omega_{\max}} d\omega\sqrt{k^2+\omega^2}\,e^{-t\sqrt{k^2+\omega^2}}\left(\frac{\gamma\,\text{Area}}{2\pi}-\frac{\text{Perimeter}}{4\pi}\right)+\frac{C}{48\pi t^2}\,, \tag{23}$$

where the area and the perimeter refer to the polygonal cross section, $C=\sum_i\left(\frac{\pi}{\alpha_i}-\frac{\alpha_i}{\pi}\right)$ with α_i the interior corner angles of the polygon, and $\omega_{\max}$ is the maximal eigenvalue obtained numerically for the polygon. An additional divergent term $\ln t$ must be considered in the presence of boundary curvature. These approaches are now being applied to study the self-energy of stadium-shaped and elliptical cavities, as well as to investigate the self-energy associated with the *outside* of a billiard of arbitrary shape.

5. CONCLUSIONS

We have seen that careful regularization and renormalization (including both inside and outside contributions) are needed to obtain physically meaningful vacuum energies and Casimir forces. Classical orbit approaches, including both periodic and non-peridoic orbits, produce exact results in simple cases and may allow for good approximations where exact solutions are nonexistent, including general quantum graphs and polygonal billiards. Furthermore, such semiclassical approximations may be compared with results obtained numerically by directly summing eigenfrequencies and subtracting known divergences associated with the Weyl part of the spectrum. Intelligent combination of analytical and numerical tools can be a promising tool for furthering our understanding of Casimir forces in general geometries.

ACKNOWLEDGMENTS

This work was supported in part by the NSF under Grant No. PHY-0545390.

REFERENCES

1. H. B. G. Casimir, *Konink. Nederl. Akad. Weten., Proc. Sec. Sci.* **51**, 793–795 (1948).
2. K. A. Milton, *The Casimir Effect: Physical Manifestations of Zero-Point Energy*, World Scientific, Singapore, 2001.
3. C. M. Bender and P. Hays, *Phys. Rev. D* **14**, 2622–2632 (1976).

4. E. Elizalde, *J. Phys. A* **40**, 6647 (2007).
5. E. Elizalde, S. Nojiri, S. D. Odintsov, and S. Ogushi, *Phys. Rev. D* **67**, 063515 (2003).
6. H. B. Chan, V. A. Aksyuk, R. N. Kleiman, D. J. Bishop, and F. Capasso, *Science* **291**, 1941–1944 (2001).
7. P. Kuchment, in *Analysis on Graphs and its Applications*, Proc. Symp. Pure. Math., AMS 2008, pp. 291–314.
8. T. Kottos and U. Smilansky, *Ann. Phys. (N.Y.)* **274**, 76 (1999).
9. P. Kuchment, *Waves Random Media* **14**, S107 (2004).
10. G. Berkolaiko, J M. Harrison, and J H. Wilson, *J. Phys. A: Math. Theor.* **42**, 025204 (2009).
11. S. A. Fulling, L. Kaplan, and J. H. Wilson, Phys. Rev. A **76**, 012118 (2007).
12. R. M. Cavalcanti, *Phys. Rev. D* **69**, 065015 (2004).
13. Z. H. Liu, Ph.D. dissertation, Texas A&M University, 2009.
14. S. A. Fulling, L. Kaplan, K. Kirsten, Z. H. Liu, and K. A. Milton, *J. Phys. A* **42**, 155402 (2009).
15. W. Lukosz, *Physica* **56**, 109 (1971).
16. E. K. Abalo, K. A. Milton, and L. Kaplan, arXiv:1008.4778.